

## Angular Distribution of Molecular $K$ -Shell Auger Electrons: Spectroscopy of Photoabsorption Anisotropy

Dan Dill and John R. Swanson

*Department of Chemistry, Boston University, Boston, Massachusetts 02215*

and

Scott Wallace

*Center for Materials Science and Engineering, Massachusetts Institute of Technology, Cambridge, Massachusetts 02139*

and

J. L. Dehmer

*Argonne National Laboratory, Argonne, Illinois 60439*

(Received 15 November 1979)

The angular distribution of Auger electrons emitted in the decay of molecular  $K$ -shell vacancies created by photoabsorption is predicted to be a direct probe of the anisotropy of molecular photoabsorption. The  $\sigma \rightarrow \pi$  discrete absorption and the  $\sigma \rightarrow \sigma f$ -wave shape resonance in  $N_2$  and CO are given as examples.

PACS numbers: 33.80.Eh

Atomic  $K$ -shell vacancies are isotropic and hence electrons emitted by Auger decay of such vacancies have an isotropic angular distribution.<sup>1-4</sup> Molecules are different, however, for two reasons. First, molecular photoabsorption is highly anisotropic, both in the discrete, because excited states have definite symmetries but generally different energies, and in the continuum, where shape resonances can enhance photoabsorption along characteristic directions of the molecule.<sup>5-9</sup> As a result, molecular photoabsorption produces neutral-molecular excited states with definite, characteristic orientations and shape-resonant photoionization produces molecular ions with energy-dependent orientations characteristic of each resonance. Second, subsequent decay of the  $K$ -shell vacancy is a fast process compared with molecular rotation, so that the orientation of the molecular excited state/ion will be reflected in the angular distribution of the emitted Auger electrons. For example, in

CO and  $N_2$  there is a very intense discrete absorption of  $\pi$  symmetry about 1 Ry below the  $K$ -shell ionization threshold and a broad  $\sigma$ -symmetry shape resonance centered about 1 Ry above threshold.<sup>6,7,10</sup> The photoabsorption to the  $\pi$  excited states preferentially creates excited molecules perpendicular to the electric vector of the light while photoionization within the  $\sigma$  shape resonance yields molecular ions preferentially parallel. The angular distribution of a particular Auger electron will mirror these alternative orientations as one scans through the photoabsorption spectrum. Thus, molecular Auger-electron angular distributions, as a function of photoexcitation energy, provide us with a spectroscopy of the anisotropy of molecular photoabsorption. This spectroscopy permits an identification of the symmetry of discrete excited states as well as a symmetry decomposition of continuum states.

For randomly oriented molecules in the gas phase, the molecular orientation induced by photoabsorption is given by Eq. (13) of Ref. 11 as

$$d\sigma_m^{m_p}/d\Omega_m = \frac{1}{3}\pi\alpha h\nu(4\pi)^{1/2} \sum_{K=0}^2 \sum_{M=0}^K (2K+1)^{-1/2} \text{Re}[Z_{KM}^{m_p}(\nu)Y_{KM}(\theta_m, \varphi_m)], \quad (1)$$

in terms of the azimuthal and polar angles  $\Omega_m = (\theta_m, \varphi_m)$  of the molecule with respect to the laboratory coordinates, with  $z$  axis along the electric vector for linearly polarized light ( $m_p = 0$ ) or along the propagation direction for left- and right-circularly polarized light ( $m_p = \pm 1$ ). The maximum harmonic  $K = 2$  reflects the dipole character of the photoabsorption. The dynamics of the molecu-

lar orientation is contained in the coefficients  $Z$ , which depend on the photon energy  $h\nu$ . Explicit expressions for them in terms of photoabsorption dipole amplitudes are given in Ref. 11. If we denote by  $d^2P_a/d\hat{k}_a d\Omega_m$  the probability of Auger emission along the direction  $\hat{k}_a$ , with the molecule oriented along  $\Omega_m$ , then the basic expression

for the Auger-electron angular distribution can be written

$$\frac{dP_a^{m_p}(\nu)}{d\hat{k}_a} = \frac{1}{\sigma_m(\nu)} \int d\Omega_m \frac{d\sigma_m^{m_p}(\nu)}{d\Omega_m} \frac{d^2P_a}{d\hat{k}_a d\Omega_m}. \quad (2)$$

Here we make the assumption that  $\Omega_m$  changes negligibly between creation of the  $K$ -shell vacan-

$$\frac{dP_a^{m_p}(\nu)}{d\hat{k}_a} = \frac{2\pi}{\hbar} (4\pi)^{-1} \sum_K P_K(\cos\theta_a) \sum_{\substack{l, l', \\ m' = m}} (-1)^{K(l', 0; K, 0 | l, 0)} (l, m; K, m' - m | l', m')$$

in terms of complex amplitudes<sup>4</sup>

$$M_{a,L}^- = i^{-l} \exp(i\sigma_l) \langle \Psi_{a,L}^- | V_C | \Psi_m \rangle \quad (4)$$

for Auger decay by Coulomb interaction  $V_C$  of the molecular excited state or ion  $\Psi_m$  to the Auger state  $\Psi_a^-$ , normalized with incoming-wave boundary conditions (denoted by the superscript “-”) appropriate to the Auger electron ejected along  $\hat{k}_a$ , with kinetic energy  $k_a^2$ , Coulomb phase  $\sigma_l$ , and asymptotic orbital momentum  $l$  and projection  $m$  along the molecular  $z$  axis, denoted as  $L = (l, m)$ . The key result here is that, while the harmonic composition of the angular distribution (3) depends on the orbital momenta of the Auger electrons, through the Clebsch-Gordan coefficients, *each harmonic is directly proportional to the corresponding harmonic in the orientation (1) of the excited molecules*, through the coefficients  $Z_{KM}$ . In particular, the maximum harmonic of the angular distribution (3) can be no greater than  $K = 2$ , because of the dipole nature of the photoabsorption.

To illustrate these results we can apply them to photoabsorption in  $N_2$  and CO. Because these molecules are cylindrically symmetric, all harmonics of the molecular orientation vanish except  $K = 0$  and  $K = 2$ ,  $M = 0$ , and Eq. (1) then takes the particularly simple form (here we choose linear polarization,  $m_p = 0$ )<sup>11, 14</sup>:

$$d\sigma_m(\nu)/d\Omega_m = \sigma_m(\nu)/4\pi [1 + \beta_m(\nu)P_2(\cos\theta_m)]. \quad (5)$$

$$dP_a^{m_p}(\nu)/d\hat{k}_a = (P_a/4\pi) [1 + \beta_m(\nu)c_a^{m_p}P_2(\cos\theta_a)], \quad (7)$$

showing the direct connection with  $\beta_m$ , i.e., the asymmetry of molecular orientation following photoabsorption. The constant  $c_a$  is characteristic of each Auger decay and independent of photoexcitation energy. It is given by

$$c_a^{m_p} = \frac{1}{2}(2 - 3m_p^2) \sum_{l, l'} (l', 0; 2, 0 | l, 0) (l, \lambda_a; 2, 0 | l, \lambda_a) \text{Re} [M_{a, l, \lambda_a}^{-*} M_{a, l, \lambda_a}^-] / \sum_l |M_{a, l, \lambda_a}^-|^2, \quad (8)$$

cy and its subsequent decay by Auger emission. This is reasonable since Auger widths are typically 0.2–1 eV<sup>12</sup> while rotational spacings are typically 0.001 eV. This is analogous to the axial-recoil approximation used in photofragment angular-distribution theory.<sup>13, 14</sup> We also treat the photoionization and Auger decay as independent processes.<sup>4</sup> As we show in detail elsewhere,<sup>15</sup> Eq. (2) can be written as

$$\times \text{Re} \{ [Z_{K, m' - m}^{m_p}(\nu)/Z_{00}^{m_p}(\nu)] M_{a, L}^{-*} M_{a, L}^- \} \quad (3)$$

The asymmetry parameter measures the difference between the photoabsorption strengths  $D_{\lambda^2}$  for molecular orientation along ( $\sigma$ ) or perpendicular to ( $\pi$ ) the electric vector of the light<sup>14</sup>:

$$\beta_m(\nu) = 2[D_{\sigma^2}(\nu) - D_{\pi^2}(\nu)]/[D_{\sigma^2}(\nu) + 2D_{\pi^2}(\nu)]. \quad (6)$$

This asymmetry parameter is complimentary to the more familiar asymmetry parameter  $\beta_e(\nu)$  characterizing the angular distribution of the photoelectron; in particular,  $\beta_e(\nu)$  contains interference terms, not present in  $\beta_m(\nu)$ , between  $\sigma$  and  $\pi$  ionization amplitudes.<sup>14</sup> The allowed range of  $\beta_m$  extends from 2 (oriented along the electric vector), through 0 (no orientation), to -1 (orientation perpendicular to the electric vector). Equation (6) is the basis of the intuitive results stated earlier: For discrete absorption, on the one hand,  $\sigma \rightarrow \sigma$  transitions have  $\beta_m = 2$  (parallel orientation) while  $\sigma \rightarrow \pi$  transitions have  $\beta_m = -1$  (perpendicular orientation); for continuum absorption, on the other hand, the strengths  $D_{\lambda^2}$  have been calculated<sup>8</sup> in the vicinity of the  $\sigma \rightarrow \sigma$  shape resonance, using the one-electron multiple-scattering model,<sup>16, 17</sup> and the resulting asymmetry parameters  $\beta_m$  for the  $K$  shells of  $N_2$  and CO are shown in Fig. 1. Orientation along the electric vector is seen to be considerable through the shape resonance.

The Auger-electron angular distribution becomes

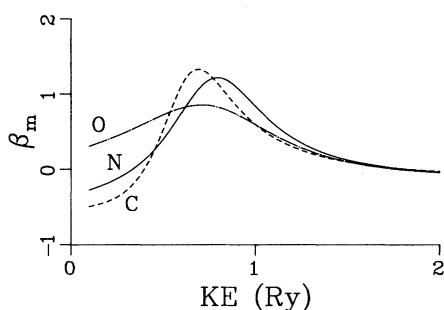


FIG. 1. Molecular orientation asymmetry parameter for photoionization of the  $K$  shells of  $N_2$  and  $CO$ , in the vicinity of the  $\sigma f$ -wave shape resonance. Electron kinetic energy is  $h\nu$  - ionization potential.

where  $\lambda_a$  is the projection (0 for  $\sigma$  or 1 for  $\pi$ ) of the Auger-electron orbital momentum, depending on the particular Auger transition. The requirement that Eq. (7) be nonnegative restricts  $c_a$  to the range  $-\frac{1}{2}$  to 1. Equation (8) can be interpreted as the relative contribution to the angular distribution of the Auger electron, in the molecular frame, of the harmonic  $K=2, M=0$ . Because molecular charge distributions are highly anisotropic, the  $c_a$  can be expected to be nonzero in general. Their evaluation requires direct calculation of the Auger amplitudes (4), except in the special case that only a single orbital momentum contributes, for which Eq. (8) is easily evaluated analytically. Alternatively, they can be determined by measuring Eq. (7) for a discrete absorption of known symmetry, or from fitting Eq. (7) across a shape resonance by use of the (in general easier to calculate) molecular asymmetry parameter (6).

A key aspect of the result in Eq. (7) is that the effect is expected for any Auger transition filling the  $K$ -shell vacancy. That is, the effect probes not only the intrinsic anisotropy of the Auger process (though there must be some anisotropy, i.e.,  $c_a$  must be nonzero) but rather the anisotropy in the creation of the  $K$ -shell vacancy. The  $KLL$  Auger spectra of  $N_2$  and  $CO$  have been analyzed in detail by Moddeman *et al.*<sup>18</sup> and show many lines which should be accessible to study. For example, in  $N_2$  there is a series of strong lines with Auger electron kinetic energies from 367–359 eV. In  $CO$  there are similar series of lines from 254–246 eV for a carbon  $K$  hole and from 500–491 eV for an oxygen  $K$  hole. These lines should show angular variation with a dependence on the frequency of the light used to create the  $K$ -shell hole determined by the mole-

cular alignment asymmetry parameter  $\beta_m$ .

We can make similar analyses for each of the molecular point groups to determine the characteristic molecular orientation for each symmetry group of discrete absorption lines and the characteristic energy dependence of each continuum shape resonance, because of the symmetry of its resonant component. (In general, for molecules without cylindrical symmetry harmonics  $K=2, M=1$ , and  $K=2, M=2$  can also contribute<sup>11</sup> and their contribution will depend on photoabsorption dynamics as well as symmetry.) Thereby, the variation of the Auger-electron angular distribution throughout a photoabsorption spectrum should allow the decomposition of that spectrum into its component molecular symmetries. For this reason, we feel that Auger-electron angular distributions provide us with a significant new molecular photoabsorption spectroscopy.

This work was performed under the auspices of the U. S. Department of Energy and was supported by the National Science Foundation under Grant No. CHE-78-08707. Acknowledgment is also made to the Donors of the Petroleum Research Fund administered by the American Chemical Society for partial support of this work.

<sup>1</sup>W. Mehlhorn, *Phys. Lett.* **26A**, 166 (1968).

<sup>2</sup>B. Cleff and W. Mehlhorn, *Phys. Lett.* **37A**, 3 (1971).

<sup>3</sup>S. Flugge, W. Mehlhorn, and V. Schmidt, *Phys. Rev. Lett.* **29**, 7 (1972).

<sup>4</sup>B. Cleff and W. Mehlhorn, *J. Phys. B* **7**, 593 (1974).

<sup>5</sup>J. L. Dehmer, *J. Chem. Phys.* **56**, 4496 (1972), and references therein.

<sup>6</sup>J. L. Dehmer and D. Dill, *Phys. Rev. Lett.* **35**, 313 (1975).

<sup>7</sup>J. L. Dehmer and D. Dill, *J. Chem. Phys.* **65**, 5327 (1976).

<sup>8</sup>D. Dill, S. Wallace, J. Siegel, and J. L. Dehmer, *Phys. Rev. Lett.* **41**, 1230 (1978), and **42**, 411(E) (1979).

<sup>9</sup>S. Wallace, Ph.D. thesis, Boston University, 1979 (unpublished).

<sup>10</sup>G. R. Wight, C. E. Brion, and M. J. van der Wiel, *J. Electron Spectrosc. Relat. Phenom.* **1**, 457 (1973); R. B. Kay, Ph. E. van der Leeuw, and M. J. van der Wiel, *J. Phys. B* **10**, 2513 (1977).

<sup>11</sup>S. Wallace and D. Dill, *Phys. Rev. B* **17**, 1692 (1978).

<sup>12</sup>W. Bambynek, B. Crasemann, R. W. Fink, H. U. Freund, H. Mark, C. D. Swift, R. E. Price, and P. V. Rao, *Rev. Mod. Phys.* **44**, 716 (1972); M. O. Krause, *J. Phys. Chem. Ref. Data* **8**, 329 (1979).

<sup>13</sup>R. N. Zare, *Mol. Photochem.* **4**, 1 (1972).

<sup>14</sup>J. L. Dehmer and D. Dill, *Phys. Rev. A* **18**, 164 (1978).

<sup>15</sup>D. Dill, J. R. Swanson, S. Wallace, and J. L. Dehmer, to be published.

<sup>16</sup>D. Dill and J. L. Dehmer, *J. Chem. Phys.* **61**, 692 (1974).

<sup>17</sup>J. L. Dehmer and D. Dill, in *Electron Molecule and Photon Molecule Collisions*, edited by V. McKoy,

T. Rescigno, and B. Schneider (Plenum, New York, 1979), pp. 225-265.

<sup>18</sup>W. E. Moddeman, T. A. Carlson, M. O. Krause, and B. P. Pullen, *J. Chem. Phys.* **55**, 2317 (1971).

## Schwinger Variational Principle for Multichannel Scattering

Kazuo Takatsuka and Vincent McKoy

*Arthur Amos Noyes Laboratory of Chemical Physics, California Institute of Technology,  
Pasadena, California 91125*

(Received 20 March 1980)

This Letter presents the first application of the Schwinger variational principle for multichannel scattering. Results are presented for an exactly soluble two-channel model problem. The accuracy and convergence of the Schwinger variational principle are shown to be extremely good and superior to those of other variational methods.

PACS numbers: 34.80.-i, 34.50.-s, 34.10.+x

In spite of several desirable features, the Schwinger variational principle<sup>1,2</sup> has not been applied extensively to scattering problems. Several recent applications<sup>3-7</sup> of the Schwinger principle to single-channel electron-molecule collision problems demonstrated the potential of the Schwinger method. Furthermore, we are currently extending the Schwinger method to multichannel problems on the basis of a new formulation. In order to assess the effectiveness and accuracy of the Schwinger method for multichannel cases, we have solved the model two-channel problem proposed by Huck<sup>8</sup> prior to its application to actual systems. In this application, we have found that the Schwinger method is extremely effective yielding results far more striking than those of sophisticated versions of the standard variational principles.<sup>9-12</sup> As far as we know, this is the first example of the application of the Schwinger principle to a multichannel problem.

The exactly soluble two-channel model problem used by Huck,<sup>8</sup> Nesbet,<sup>9-11</sup> and more recently by Harris,<sup>12</sup> is defined by the Hamiltonian  $H = H_0 + V$  with

$$H_0 = |\chi_1\rangle \left(-\frac{1}{2}d^2/dr^2\right) \langle\chi_1| + |\chi_2\rangle \left[-\frac{1}{2}d^2/dr^2 + \Delta E\right] \langle\chi_2|, \quad (1)$$

and

$$V = \sum_{m \neq n}^2 |\chi_m\rangle V_{mn} \langle\chi_n|, \quad (2)$$

where

$$V_{12} = V_{21} = \begin{cases} \frac{1}{2}C, & r < a \\ 0, & r > a, \end{cases} \quad (3)$$

and  $\langle\chi_m|\chi_n\rangle = \delta_{mn}$ . In terms of the regular eigenfunctions of  $H_0$ ,

$$S_m(r_1, r_2) = \chi_m(r_1) k_m^{-1/2} \sin k_m r_2, \quad m = 1, 2, \quad (4)$$

the variational functional for the  $K$  matrix is given by

$$[K_{mn}] = \frac{\langle\Psi_m|U|S_n\rangle \langle S_m|U|\Psi_n\rangle}{\langle\Psi_m|(UG_0U - U)|\Psi_n\rangle}, \quad (5)$$

where  $U = 2V$ . In Eq. (5), the free-particle (standing-wave) Green's function  $G_0$  is

$$G_0(r_1, r_2; r_1', r_2') = -\sum_{m=1}^2 S_m(r_1, r_<) C_m(r_1', r_>), \quad (6)$$

where  $C_m$  is the irregular solution of  $H_0$ , and  $r_> = \max(r_2, r_2')$  and  $r_< = \min(r_2, r_2')$ . It should be noted that the above Green's function has a very simple structure, since no permutation symmetry is imposed on the wave functions  $\Psi_m$  ( $m = 1, 2$ ). As usual, the wave function is expanded in terms of a basis set  $\{\eta_i^m | m = 1, 2; i = 1, \dots, N\}$ . From the stationary condition  $\delta[K_{mn}] = 0$ , the  $K$ -matrix elements can be written as

$$K_{mn} = \sum_{a,b}^2 \sum_{i,j}^N \langle S_m|U|\eta_i^a\rangle D_{ij}^{ab} \langle\eta_j^b|U|S_n\rangle, \quad (7)$$

where

$$(D^{-1})_{ij}^{ab} = \langle\eta_i^a|(UG_0U - U)|\eta_j^b\rangle. \quad (8)$$

In order to compare with the previous results of Nesbet *et al.*<sup>9-11</sup> and Harris and Michels<sup>12</sup> and the exact results,<sup>9</sup> we also choose the potential parameters  $a = 1.0$  and  $C^2 = 10.0$ , and the energies